Journal of Hazardous Materials, 13 (1986) 353—367
Elsevier Science Publishers B.V., Amsterdam — Printed in The Netherlands

SORPTION—DESORPTION PHENOMENA OF CHEMICALS FROM POLYMER (PAINT) FILMS

A.D. SCHWOPE, J. KLEIN*, K.R. SIDMAN and R.C. REID**

Arthur D. Little, Inc., Acorn Park, Cambridge, MA 02140 (U.S.A.)
**U.S. Army Chemical Research and Development Center, Aberdeen Proving Ground, MD 21020 (U.S.A.)*
***Department of Chemical Engineering, Massachusetts Institute of Technology, Cambridge, MA 02139 (U.S.A.)*
(Received October 15, 1985; accepted January 16, 1986)

Summary

The sorption and later desorption of a toxic chemical from polymers and, more specifically, paint films represent a potential hazard to personnel in proximity to these contaminated surfaces. Such hazards may be due to resultant vapor concentrations or to direct transfer of the chemical to the skin upon touching the surface. Desorption rates are dependent on the properties of the chemical/polymer pair, boundary conditions, partition coefficient, and the initial concentration profile in the material. The initial concentration profile is dependent on the diffusion coefficient and solubility of the chemical in the polymer as well as the duration of the contamination period. An analytical model is developed to predict desorption fluxes on the basis of the contamination scenario, the conditions external to the contaminated material and physical properties as determined by independent tests. The model predicted well the desorption of diethyl malonate, a toxic chemical simulant, from alkyd paint films.

Introduction

Polymeric materials, in contrast to glass and most metals, will absorb chemicals from both vapor and liquid, and later desorb these chemicals. This phenomenon may lead to serious problems. One often cited example relates to the reuse of plastic beverage containers. The reuse of such containers for beverage containment is not widely practiced commercially as there is the possibility that a customer may have temporarily used the container for storage of, for example, gasoline or a pesticide. Depending on the storage time and conditions, there is the further possibility that components of such mixtures may migrate into the wall of the container. Such components may not be completely or easily removed by traditional container-cleaning processes. Upon refilling the container with fresh beverage, the sorbed components may then migrate from the container to the beverage. Not only could this result in off-taste or product degradation but also it could result in a toxicity hazard to consumers. While the probability of this event is small, it

0304-3894/86/$03.50

weighs heavily on those organizations considering the reuse of plastic beverage containers.

Another scenario would involve painted metal surfaces exposed to a toxic chemical (e.g., methyl isocyanate or a pesticide) which sorbs into the paint during the contact period. Standard surface cleaning techniques may not remove all the sorbed chemical; and some may remain in the paint film. At later times these residuals would be free to migrate from the paint film. Depending on the rate of migration and the toxicity of the chemical, such migration could represent a hazard to persons in proximity to the contaminated surface.

This paper presents the results of a study to examine, both theoretically and experimentally, the sorption and desorption of chemicals in paint films. Emphasis has been placed on alkyd paints, but some experiments were also conducted with polyurethane paints. In this study the paint is assumed to be bonded to an impermeable substrate (e.g., metal) and is exposed, uniformly, to a chemical for a period of time, τ. After this time, the source of contamination is removed and desorption allowed to occur to a stream of flowing air. The rate of chemical desorption as a function of time, t, is the variable of interest.

Models

Sorption into and diffusion within a heterogeneous medium such as a pigmented polymer (or paint) is a very complex problem. The approach often taken is to modify well-established mathematical models for sorption into homogeneous films to take into account pigment adsorption and increased path length due to the presence of the filler [1—8]. Such treatments presume a detailed picture of the heterogeneous film structure — information not normally available in practical situations.

In our model, we assumed that diffusional processes could be represented by an average *effective* diffusion coefficient and, also, that there was a finite solubility of the sorbing chemical into the paint film. We have developed a two-step model with a sorption period of duration τ followed by a desorption period of indefinite duration, t, after removal of the chemical from the surface. The model is based on Fick's laws.

The solution to Fick's law for the sorption period is well known [9], i.e. at time τ, the concentration of the chemical at any position within the polymer is

$$C(x,\tau) = C_0\left\{1 - 2\sum_{n=0}^{\infty}[(-1)^n/p_n]\cos[p_n(1-\epsilon)]\exp(-p_n^2\psi_\tau)\right\} \qquad (1)$$

where $\epsilon = x/L$ with x the distance measured in from the contaminated surface and L the paint film thickness. $p_n = (2n+1)\pi$, and ψ_τ is a dimensionless time $= D\tau/L^2$ with D the effective diffusion coefficient of the chemical in the paint film. C_0, the equilibrium surface concentration of the chemical in

the paint, is assumed invariant with time during the sorption. A further assumption is that there was no chemical in the film at $\tau = 0$.

The quantity of chemical sorbed at τ is given by integration of eqn. (1), i.e.

$$M_\tau = C_0 L \left\{ 1 - 2 \sum_{n=0}^{\infty} [\exp(-p_n^2 \psi_\tau)] / p_n^2 \right\} \tag{2}$$

For small values of ψ_τ, eqns. (1) and (2) simplify to

$$C(x,t) = C_0 \operatorname{erfc}(\epsilon / 2\psi_\tau^{1/2}) \tag{3}$$

$$M_\tau = 2C_0 L (\psi_\tau / \pi)^{1/2} \tag{4}$$

where erfc is the complementary error function.

The use of a constant (effective) diffusion coefficient in developing eqns. (1) and (2) clearly represents a major simplification, but the complex structure of most paint films with high loadings of pigment would lead to serious mathematical difficulties if one attempted to proceed by a more rigorous approach. In addition, as will be shown later, short time sorption tests with paint films did indicate that M_τ was proportional to $\psi_\tau^{1/2}$ as suggested by eqn. (4).

As noted earlier, the surface is cleansed of contaminant at time τ, at which time sorption is assumed to cease. This event could result from washing away residual liquid chemical, or by removing a source of contaminating vapor. At τ, it is then assumed that the paint film is exposed to a flow of uncontaminated air (or other gas) which can sweep any desorbing chemical diffusing to the surface. Within the paint film, using Fick's law with a constant D, it may be shown (see Appendix) that the concentration of chemical can be expressed as in eqns. (A-7) and (A-19). By differentiating eqn. (A-7) and using eqn. (A-3), the flux of chemical leaving the surface is then

$$dM_t/dt = kKC_0 \sum_{n=0}^{\infty} b_n \cos(\theta_n) \exp(-\theta_n^2 \psi_t) \tag{5}$$

Where $\theta_n = n\pi + \eta_n$ and η_n can be found from the roots of the characteristic equation

$$(R)^{-1} (n\pi + \eta_n) \sin \eta_n - \cos \eta_n = 0 \qquad 0 < \eta_n \leqslant \pi/2 \tag{6}$$

with $R = kKL/D$ and $\psi_t = Dt/L^2$. The coefficients b_n are given in eqn. (A-19). The mass transfer resistance is described through a mass transfer coefficient (k) and the partitioning of the chemical between the paint-film surface and the air boundary layer is related to a partition coefficient K, i.e.,

$$K = \frac{\text{concentration in vapor at the surface}}{\text{concentration in the paint film at the surface}} \tag{7}$$

The variable t represents the time after the sorption time τ.

There are several dimensionless groups which are important in interpreting the results from this model. The group $R = kKL/D$, used in eqn. (6), characterizes the external mass transfer resistance relative to the internal diffusion. It is important to note that the mass transfer coefficient (k) and the partition coefficient (K) always appear as a product and low values of either k or K lead to situations where external mass transfer resistances predominate. A limiting case of $R \to 0$ would indicate that there was no diffusional resistance within the paint film; conversely as $R \to \infty$, external resistances are negligible compared to internal diffusion resistances.

Results from the flux equation are discussed later when experimental data are introduced. The behavior of the calculated concentration profiles determined from eqns. (A-7) and (A-19) is illustrated in Figs. 1 and 2. Both were computed with $R = \infty$ to indicate results when external mass transfer resistances were unimportant.

In Fig. 1, a relatively thick paint film was chosen (0.25 mm). The film was presumed to be contaminated for 0.5 h (τ) and then allowed to desorb for 1.5 h. The curves show the concentration profiles within the paint film in terms of the ratio of the local concentration C to that which existed in the paint film surface during sorption, i.e., the saturation concentration, C_0. Thus at the end of the sorption period ($t = 0$), and at $x = 0$, the curve of C/C_0 would begin at 1.0 and decrease with depth as given by eqn. (1). As desorption occurs, the value of C/C_0 is maintained at zero at $x = 0$ (the surface) due to the stipulation that $R \to \infty$. At the same time, diffusion occurs toward the interior of the paint as there is a concentration gradient in this direction. Figure 1 shows the estimated concentration profiles of chemical in a paint film over a range of diffusion coefficients at a time 1.5 h after the removal of surface contamination. For low values of D, all the chemical is localized near the surface; due to this low D, little chemical was sorbed and little remains. For larger D, there is very little chemical near the interface since it is rapidly lost, but the high mobility has allowed more to be sorbed and to penetrate the paint film.

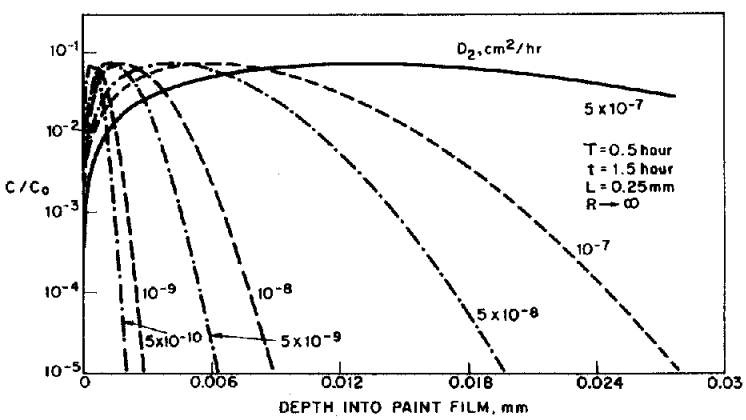

Fig. 1. Influence of diffusion coefficients on concentrations profiles.

Figure 2 illustrates the predicted changes in the concentration profiles as a function of time from the start of surface decontamination. Results for two paint film thicknesses are shown. In this case ($D = 5 \times 10^{-7}$ cm^2/h), the entire film was not saturated within the 0.5 h contamination period and a non-uniform concentration profile existed during the period immediately following surface decontamination. For example see the curves for $t = 5$ min. As the desorption time increases, profiles become more uniform due to the continued diffusion and equilibration of the chemical in the paint film. Differences in the profiles due to thickness become more apparent as time increases. At 9.5 h the concentration near the surface is higher for the thinner film than for the thicker film. The result is that the desorption flux from the thinner film is then predicted to be greater than from the thicker film. This condition will persist until the chemical in the thin film is sufficiently depleted that the gradient becomes less than that in the thicker film. This is depicted in Fig. 3.

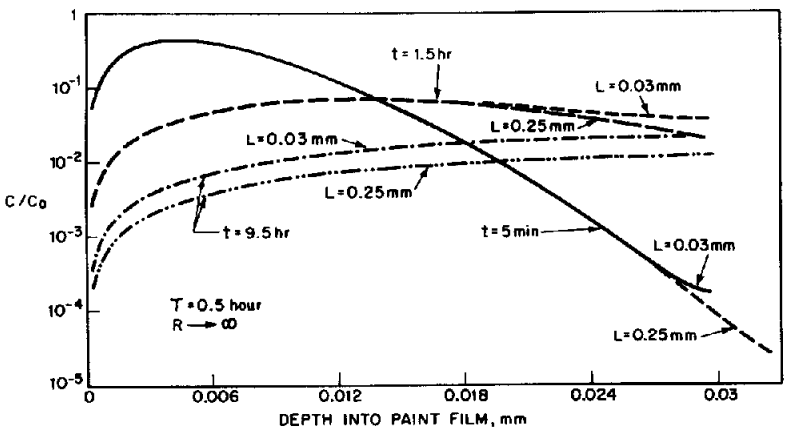

Fig. 2. Effect of paint film thickness on concentration profiles.

Other graphs could be drawn to illustrate the somewhat complex situation where there is diffusion in both directions within a film due to the desorption of material at the surface. Some of these effects will be noted later when experimental flux data are introduced.

Experimental

Most experiments were conducted with an alkyd paint produced under the government specifications given in MIL-E-52798A. The films were prepared by spraying a solution of the alkyd paint onto primed steel plates and then curing at 50°C for 115 h. The plates were then stored at 22°C, 50% relative humidity for up to 60 days. Some specimens were used directly after this treatment while others were weathered in a Weather-O-Meter for periods

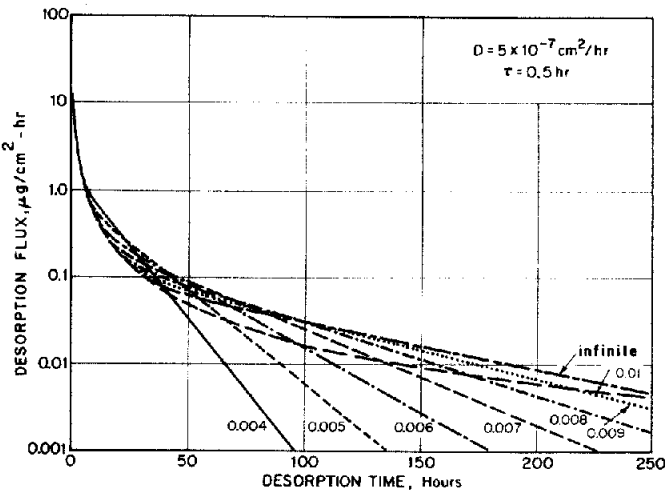

Fig. 3. Effect of film thickness on flux.

up to 400 h. Film thicknesses were measured with a micrometer and corrected for the backing plate and primer thickness. A few experiments were conducted with polyurethane paint films and, here, the results were found to be quite dependent upon the conditions of film forming, curing, and weathering. More details can be found in Sidman et al. [10].

Diethyl malonate (DEM) was chosen since it is relatively benign and it has physical properties similar to more toxic chemicals of interest to our group. DEM is a relatively nonvolatile liquid with a normal boiling point of about 199°C and a vapor pressure of about 50 Pa (0.37 torr) at 25°C.

Three types of experiments were conducted: sorption, evaporation, and sorption—desorption. In the sorption tests painted films were exposed to pure liquid DEM for various periods of time and, after surface wiping, the gain in weight due to sorption was measured. Two time regions were of particular interest, i.e., very short times and very long times. The long-time tests allowed us to determine the equilibrium solubility of DEM in the alkyd film (i.e., C_0, in the nomenclature of the model) since the mass sorbed was known as well as the film thickness and area. In the short-time experiments, DEM sorption was measured as a function of time. Equation (4) was then used to estimate the effective diffusion coefficient of DEM in the alkyd paint film since a plot of mass sorbed (per unit area) vs. the square root of time was linear with a slope of $2C_0(D/\pi)^{1/2}$. The values found for DEM in alkyd paint films, at 25°C, were $C_0 \approx 0.22$—0.23 g/cm^3 and $D \approx 2.4 \times 10^{-4}$ cm^2/h $= 7.6 \times 10^{-8}$ cm^2/s. The approximate error limits on these values are ±10—15%. Using these parameters and eqn. (4), one could match experimental M_τ values with calculated ones over a range of values of τ.

The evaporation experiments were carried out in order to obtain experi-

mental values of the external mass transfer coefficient (k) required to correlate the sorption—desorption test data. The evaporation (as well as the desorption) experiments were conducted by placing a contaminated unpainted metal specimen in a horizontal position in an enclosed tube and drawing 50% relative humidity, 25°C air over it with a vacuum system. The apparatus was calibrated to determine the superficial air flow velocities over the plate. By removing and weighing the plate at various times during the steady state evaporation period, the rate of evaporation was found. Knowing the vapor pressure of DEM at 25°C, and assuming that the bulk air contained negligible DEM, the mass transfer coefficient could be computed as a function of air velocity. For example, k = 380 cm/h at 0.35 k/h and 1900 cm/h at 8 k/h.

The desorption experiments were carried out by first contaminating alkyd-painted panels with liquid DEM at 25°C. The contamination period (τ) was, normally, 0.5 h. At this time, DEM was removed from the surface by wiping, and the panel weighed so that the total mass of DEM sorbed was known. Typical weight gains were in the range of 4 to 5 mg; the balance was accurate to within 0.1 mg. The panel was then placed in the same apparatus as used for the evaporation tests and air (50% relative humidity, 25°C) drawn over the panel. During a desorption test, the panel was removed at specified times so that the residual DEM could be determined. At long times, when all DEM had been removed, the weight of the specimens returned to their original values.

The mass desorbed—time data were plotted and slopes drawn to estimate the flux of DEM at a given time. Numerical differentiation could have been employed, but the accuracy of the data (± 10—15%) did not justify this.

One complication in the above approach was that in some cases the DEM dissolved in the paint during the sorption period to the extent that swelling of the film occurred. Thus the film thickness (L) increased. This change was measured and, often, increases of 10—20% were found. However, upon desorption, the thickness did not return to its original value. Thus, for purposes of later modelling, the *sorbed* or *swelled* thickness was chosen as the actual paint thickness.

Results and discussion

The early-time desorption fluxes measured in the tests were found to be a strong function of time in those cases where external air velocities were high, but were nearly constant over time for a significant period at low air velocities.

To explore the applicability of the analytical sorption—desorption model in correlating the experimental results, numerical values of the parameters D, C_0, k, L, and K were required. It was the objective to obtain these by *independent* measurements to avoid introducing fitted parameters into the analysis.

The effective diffusion coefficient D and the equilibrium solubility C_0 were found, as described earlier, from separate sorption tests. For DEM in the alkyd paint films used here, at 25°C, $D \approx 2.4 \times 10^{-4}$ cm^2/h and $C_0 \approx 0.225$ g/cm^3. The external mass-transfer coefficient k was measured in the independent evaporation tests noted above. L, the paint film thickness, was chosen as the *swollen* value and was determined after sorption. For the partition coefficient K, defined in eqn. (7), we assumed that the saturation concentration of DEM in the film [the denominator of eqn. (7)] was C_0. For the numerator, we selected the saturated vapor concentration of DEM in air at 1 bar and 25°C (298 K). Thus, with the ideal-gas law, this vapor concentration is $P_{vp}M/RT$ where P_{vp} is the vapor pressure of DEM at 25°C (50 Pa = 50 N/m^2), M is the molecular weight (160), and R is the gas constant. To obtain vapor concentrations in g/cm^3, $R = 8.314 \times 10^6$. Thus,

$$K = [(50)(160)/(8.314 \times 10^6)(298)]/0.225 = 1.4 \times 10^{-5}$$

With these parameters, eqns. (5), (6) and (A-19) were employed to estimate the desorption flux rates. For most experiments there was excellent agreement between predicted and measured fluxes. Two examples are shown in Figs. 4 and 5. The conditions for the data in Fig. 4 are characteristic of a test with a relatively low air velocity. Data points for two different experiments are shown to indicate the reproducibility of the results. The solid curve is computed from the model. Below flux rates of about 10 μg/cm^{2}h, the experimental uncertainty in weighing negated any possibility of obtaining

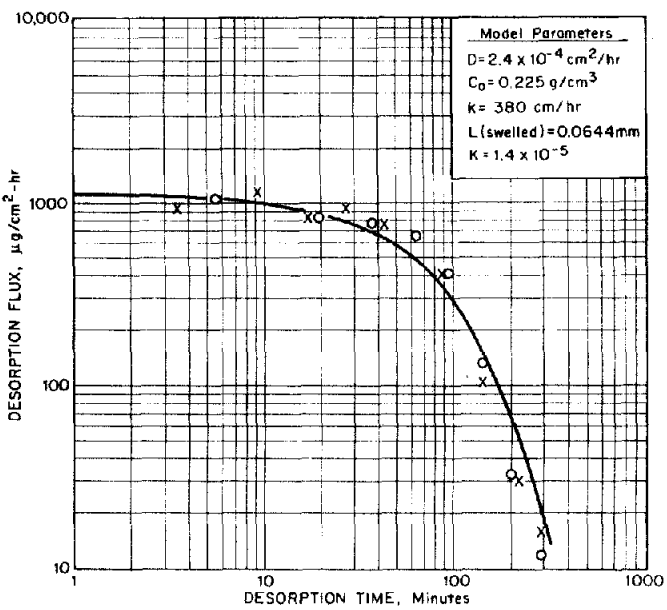

Fig. 4. DEM desorption rates from alkyd paint films at 25°C (air velocity = 0.35 k/h). Weathering time: 200 h; ○, × replicate tests.

reliable rate data. For these low air velocity tests, a significant portion of the overall mass transfer resistance resided in the vapor boundary layer in the flowing air, and this led to an almost constant desorption rate for the first 10—20 min; after this period, due to depletion of DEM in the paint layer near the surface, internal diffusional resistances began to play a more predominant role and the rate of desorption decreased.

In Fig. 5, we show the results for similar tests, but at high air velocities. Here, the external mass transfer resistance is much less and diffusional effects within the paint film are important in the early time period. Note also that by increasing the external air velocity from 0.35 to 8 k/h (10 to 220 cm/s), the desorption flux at short times increased about five-fold. In Fig. 5, one can see that there is poor agreement between the model predictions and measured flux-rates when the rates have reached a low value of about ≈ 50 $\mu g/cm^2 h$. This large scatter at low flux rates was noted in most tests — the better agreement seen in Fig. 4 being more the exception. Also, as shown in the legend in Fig. 5, the tests employed alkyd paint films which were "weathered" for different times, 200 and 400 h. As stated earlier, essentially no difference was found in the desorption rates for alkyd films weathered for various periods of time.

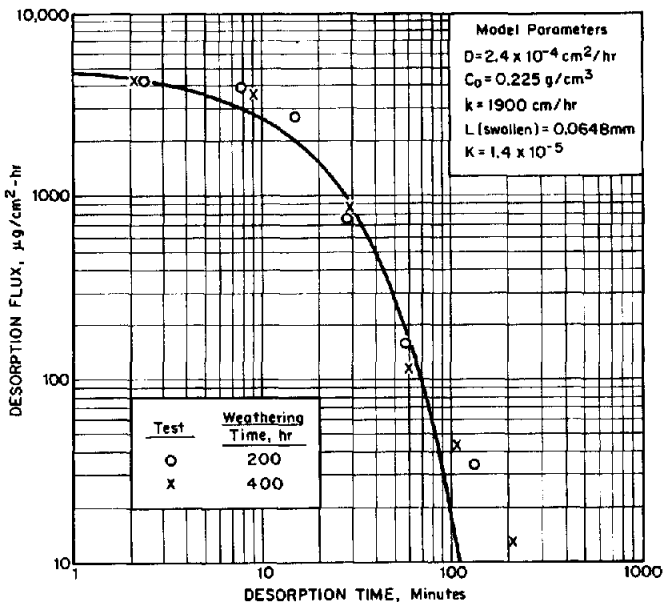

Fig. 5. DEM desorption rates from alkyd paint films at 25°C (air velocity = 8 k/h).

The data in Fig. 5 are replotted in a different manner in Fig. 6. Here the actual loss of DEM (not a flux) is graphed as a function of the square root of the desorption time. The solid curve represents the integration of eqn. (5):

$$M_t = C_0 LR \sum_{n=0}^{\infty} b_n(\cos\theta_n)\{[1 - \exp(-\theta_n^2 \psi_t)]/\theta_n^2\} \quad (8)$$

For this test, the sorption period was such as to essentially saturate the paint film before desorption began. Thus the initial loading of DEM in the film was $C_0 L = (0.225)(6.48 \times 10^{-3}) = 1.46 \times 10^{-3}$ g/cm^2. As one may note, this value is approached asymptotically at long times.

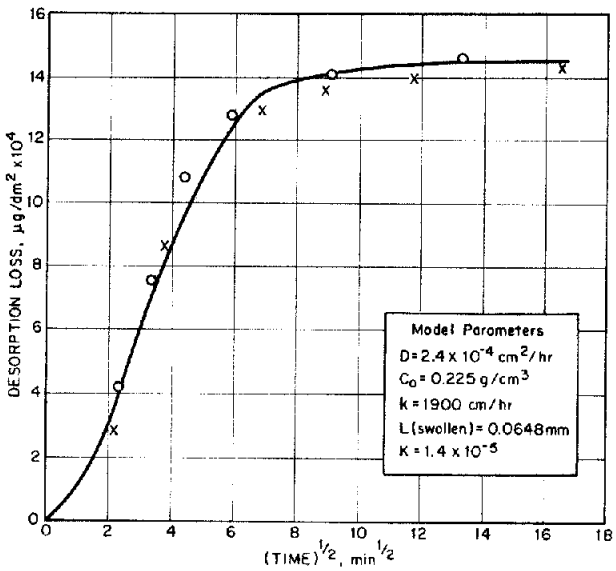

Fig. 6. Desorption of DEM from alkyd paint films at 25°C (air velocity = 8 k/h). Weathering time: ○, 200 h; ×, 400 h.

There are few data in the literature to test the model developed in this work. Thompson [11] studied the sorption—desorption of chemical warfare agents with various paint films. He employed an alkyd paint similar to that used in the present study (government specification TT-E-527) and contaminated it with liquid chemicals. After washing with alcohol and drying, the painted surface was then exposed to flowing air. The desorbed chemical was trapped and measured. While the flow conditions were not well characterized, an external mass transfer coefficient can be approximated from his data as k = 1000 cm/h. Many tests were made with 2,2'-dichloroethyl sulfide which has a vapor pressure of about 15 Pa (0.11 torr) at 25°C. Using the published equilibrium saturation concentration of this chemical in the alkyd paint, eqn. (7) was then employed to determine K. Swollen paint film thicknesses were estimated and D left as an adjustable parameter. In Fig. 7, we show some of his results at 25°C and, on the same graph, have plotted the results of the model proposed in this paper. The fitted parameter, D, was found to be about 2.2×10^{-6} cm^2/h. The other model parameters used are shown on

the graph. Whereas the flux values may appear low, for very toxic chemicals such as are of concern here, even these fluxes can be hazardous. Clearly, for the test results in Fig. 7, even at the lowest fluxes shown, the painted surface would still be releasing toxic chemical at rates which could be harmful.

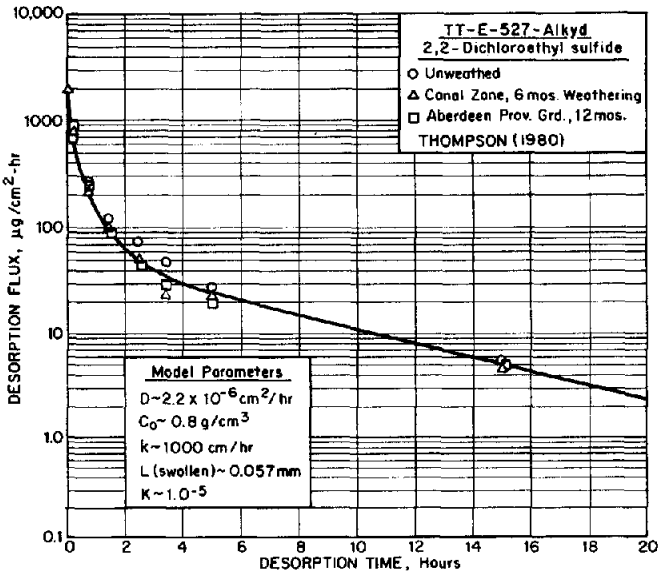

Fig. 7. Desorption fluxes of 2, 2′-dichloroethyl sulfide from alkyd paint films.

Conclusions

A new, explicit analytical model has been developed to apply to the situation wherein a polymer (or paint film) exposed to a vapor or liquid chemical is then decontaminated by desorption into a flowing gas stream. A number of assumptions were made in the development which are difficult, if not impossible to defend — such as a "constant" penetrant diffusivity and a partition coefficient independent of concentration. Also, the experimental tests involved paint films heavily loaded with pigment, yet the film was "assumed" homogeneous. Our ultimate defense is that the results of the rather complex analytical model did predict desorption fluxes in reasonable agreement with experimental data, and all parameters entering the model were found from independent measurements, i.e., no adjustable parameters were employed.

In addition, the use of the model has provided both a quantitative and qualitative appreciation of this complex, real problem. The model would be particularly advantageous in designing protocols and for interpreting experimental data — in a real-time mode. It was also shown that the fluid-mechanics

of the desorbing gas stream were often dominant in limiting desorption fluxes from the paint film, yet the literature often neglects this variable completely by providing little or no characterization of the air stream to which fluxes are measured.

Finally, whereas we have emphasized alkyd paint films in this study, some experiments were also conducted with polyurethane paint (PUP) films. For the cases studied we found that the PUP sorbed significantly less chemical than did the alkyd films. Furthermore we found that the sorption/desorption data were not consistent with the proposed solution—diffusion model. It is hypothesized that sorption into the PUP occurred by a capillary wicking mechanism; the PUP was near the critical pigment-to-volume ratio. Further investigation of PUP/chemical interactions would be desirable.

List of symbols

b_n coefficient for a series, given in eqn. (A-19)
C concentration of the chemical in the paint film
C_0 equilibrium solubility of the chemical in the paint film
D diffusion coefficient of the chemical in the paint film
k external mass transfer coefficient
K partition coefficient, defined in eqn. (7)
L swollen thickness of the paint film
M molecular weight
M_τ amount of chemical sorbed in time τ per unit area
M_t amount of chemical desorbed in time t per unit area
P_{vp} vapor pressure
R gas constant
t desorption time
T absolute temperature
x distance measured into the film

Greek Symbols

η_n parameter defined in eqn. (6)
θ_n $n\pi + \eta_n$
ϵ $(x/L$
τ sorption time
ψ_τ $D\tau/L^2$
ψ_t Dt/L^2

References

1 W.K. Asbeck and M. Van Loo, Critical pigment volume relationships, Ind. Eng. Chem., 41 (1949) 1470.
2 R.M. Barrer, J.A. Barrie and M.G. Rogers, Heterogeneous membranes: Diffusion in filled rubber, J. Poly. Sci., Part A, 1 (1963) 2565.

3 H.H. Frisch, Diffusion in inhomogeneous films and membranes, J. Membrane Sci., 3 (1978) 149.
4 W. Funke, U. Zorll and B.G.K. Murthy, Interfacial Effects in Solid Paint Films Related to Some Film Properties, J. Paint Tech. 41 (1969) 210.
5 T.K. Kwei, Polymer-filled interaction. Thermodynamic Calculations and a Proposed Model, J. Poly. Sci., Part A, 3 (1965) 3229.
6 T.K. Kwei and C.A. Kumins, Polymer-filler interaction: Vapor sorption studies, J. Polym. Sci., 8 (1964) 1483.
7 G.S. Park, Transport in polymer films, in: R.R. Myers and J.S. Long (Eds.), Treatise on Coating 2, Part II, Marcel Dekker, NY, 1976, Chap. 9.
8 C.M. Peterson, Permeability studies on heterogeneous polymer films, J. Appl. Polym. Sci., 12 (1968) 2649.
9 J. Crank, The Mathematics of Diffusion, 2nd. edn., Clarendon Press, Oxford, 1975.
10 K.R. Sidman, A.D. Schwope, W.D. Steber and R.C. Reid, Absorption and Desorption of Organic Liquids by Paint Films, A.D. Little, Inc., Cambridge, MA, AD410 613L, October 1982.
11 J.H. Thompson, CRDC, personal communication, 1985.
12 C. Lonczos, Discourse on Fourier Series, Hafner Pub. Co., NY, 1966, p. 75.
13 H. Margenau and G.M. Murphy, The Mathematics of Physics and Chemistry, D. van Nostrand Co., NY, 1943, p. 253.

Appendix

We assume Fick's law, with a constant diffusion coefficient, applies for the chemical diffusing from the interior to the surface and desorbing.

$$\partial C(x,t)/\partial t = D[\partial^2 C(x,t)/\partial x^2] \tag{A-1}$$

The initial condition, $t = 0$ (i.e., after the period τ), is given by eqn. (1), and the boundary conditions are

$$D[\partial C(L,t)/\partial x] = 0 \tag{A-2}$$

$$D[\partial C(0,t)/\partial x] = kKC(0,t) \tag{A-3}$$

Equation (A-2) states that the concentration gradient at $x = L$ (the film—substrate interface) is zero. Equation (A-3) states that the flux of chemical leaving the film into the environment must equal the mass transfer flux. The latter is given as a product of the mass transfer coefficient (k) and the chemical concentration in the environment, at the interface, $[KC(0,t)]$.

A solution to eqn. (A-1) which satisfies eqn. (A-2) is given by

$$f_n = b_n \cos[\theta_n(1-\epsilon)] \exp(-\theta_n^2 \psi_t) \tag{A-4}$$

where ϵ is x/L and $\psi_t = Dt/L^2$

To satisfy eqn. (A-3), the following relationship must be valid

$$\theta_n \sin\theta_n = R \cos\theta_n \tag{A-5}$$

where $R = kKL/D$. Equation (A-5) may then be rewritten as

$$\theta_n = R \cot\theta_n \tag{A-6}$$

From the Sturm—Liouville theorem, the cos functions in eqn. (A-4) form a complete orthogonal set in the interval $0 \leqslant \epsilon \leqslant 1$. Thus the solution to the chemical concentration profile is given by eqn. (A-7) [12,13].

$$C(x,t) = C_0 \sum_{n=0}^{\infty} b_n \cos[\theta_n(1-\epsilon)] \exp(-\theta_n^2 \psi_t) \tag{A-7}$$

The coefficients b_n must be such as to satisfy the equation

$$\sum_{n=0}^{\infty} b_n \cos[\theta_n(1-\epsilon)] =$$

$$1 - 2\sum_{m=0}^{\infty} [(-1)^m / p_m] \cos[p_m(1-\epsilon)] \exp(-p_m^2 \psi_\tau) \tag{A-8}$$

Multiplying both sides of eqn. (A-8) by $\cos[\theta_\nu(1-\epsilon)]$ and integrating with respect to ϵ from 0 to 1,

$$b_\nu \int_0^1 \cos^2[\theta_\nu(1-\epsilon)]\,d\epsilon = \int_0^1 \cos[\theta_\nu(1-\epsilon)]\,d\epsilon$$
$$- 2\sum_{m=0}^{\infty} [(-1)^m / p_m] \exp(-p_m^2 \psi_\tau) \int_0^1 \cos[\theta_\nu(1-\epsilon)] \cos[p_m(1-\epsilon)]\,d\epsilon \tag{A-9}$$

For the first integral, replacing the subscript ν by n,

$$\int_0^1 \cos^2[\theta_n(1-\epsilon)]\,d\epsilon = -(1/2)[1 + \sin(2\theta_n)/2\theta_n] \tag{A-10}$$

For the next integral,

$$\int_0^1 \cos[\theta_n(1-\epsilon)]\,d\epsilon = -(\sin\theta_n)/\theta_n \tag{A-11}$$

For the third integral, we note the identity,

$$(\cos\alpha)(\cos\beta) = (1/2)[\cos(\alpha+\beta) + \cos(\alpha-\beta)] \tag{A-12}$$

Also define $\epsilon' = 1 - \epsilon$ so that

$$\int_0^1 \cos(\theta_n(1-\epsilon)] \cos[p_m(1-\epsilon)]\,d\epsilon = -\int_0^1 \cos(\theta_n\epsilon') \cos(p_m\epsilon')d\epsilon'$$
$$= -I_{mn} \tag{A-13}$$

where

$$I_{mn} = (1/2)\int_0^1 \cos[(\theta_n + p_m)\epsilon']\,d\epsilon' + (1/2)\int_0^1 \cos[(\theta_n - p_m)\epsilon']\,d\epsilon'$$

$$= (1/2)\{\{[\sin(\theta_n + p_m)]/(\theta_n + p_m)\} + \{[\sin(\theta_n - p_m)]/(\theta_n - p_m)\}\} \tag{A-14}$$

As $p_m = (2m + 1)\pi/2$, $\cos p_m = 0$ and $\sin p_m = (-1)^m$,

$$I_{mn} = [(-1)^m(\cos\theta_n)/2]\{[1/(\theta_n + p_m)] - [1/(\theta_n - p_m)]\}$$

$$I_{mn} = p_m(-1)^{m+1}[\cos\theta_n/(\theta_n^2 - p_m^2)] \tag{A-15}$$

To simplify, let

$$\theta_n = n\pi + \eta_n \tag{A-16}$$

so

$$I_{mn} = (-1)^{m+n+1} p_m [(\cos\eta_n)/(\theta_n^2 - p_m^2)] \tag{A-17}$$

The transform used in eqn. (A-16) may also be employed in eqns. (A-10) and (A-11).

Returning to eqn. (A-9) and substituting with eqns. (A-10), (A-11), (A-13), and (A-17),

$$(b_n/2)[1 + (\sin 2\eta_n)/2\theta_n] = (-1)^n\{[(\sin\eta_n)/\theta_n]$$

$$+ 2\cos\eta_n \sum_{m=0}^{\infty} [\exp(-p_m^2\psi_\tau)]/(\theta_n^2 - p_m^2)\} \tag{A-18}$$

or solving for b_n,

$$b_n = (-1)^m [4\theta_n/(2\theta_n + \sin 2\eta_n)]\{[(\sin\eta_n)/\theta_n]$$

$$+ 2\cos\eta_n \sum_{m=0}^{\infty} [\exp(-p_m^2\psi_\tau)]/(\theta_n^2 - p_m^2)\} \tag{A-19}$$

Equation (A-7) with the coeffieients b_n given by eqn. (A-19) completes the solution. To obtain the flux of chemical from the surface, we use eqn. (A-7) with (A-3) to obtain values of dM_t/dt in eqn. (5).